

See discussions, stats, and author profiles for this publication at: <https://www.researchgate.net/publication/45280432>

Adsorption of a wormlike polymer in a potential well near a hard wall: Crossover between two scaling regimes

ARTICLE *in* THE JOURNAL OF CHEMICAL PHYSICS · JULY 2010

Impact Factor: 2.95 · DOI: 10.1063/1.3452322 · Source: PubMed

CITATIONS

5

READS

9

4 AUTHORS, INCLUDING:



Mingge Deng

Brown University

18 PUBLICATIONS 145 CITATIONS

SEE PROFILE



Ying Jiang

Beihang University(BUAA)

23 PUBLICATIONS 288 CITATIONS

SEE PROFILE



Haojun Liang

University of Science and Technology of China

152 PUBLICATIONS 2,247 CITATIONS

SEE PROFILE

Adsorption of a wormlike polymer in a potential well near a hard wall: Crossover between two scaling regimes

Mingge Deng,¹ Ying Jiang,² Haojun Liang,¹ and Jeff Z. Y. Chen^{2,a)}

¹CAS Key Laboratory of Soft Matter Chemistry and Hefei National Laboratory for Physical Sciences at Microscale, University of Science and Technology of China, Hefei, Anhui 230026, People's Republic of China

²Department of Physics and Astronomy, University of Waterloo, Waterloo, Ontario N2L 3G1, Canada

(Received 23 February 2010; accepted 21 May 2010; published online 19 July 2010)

We consider the adsorption of a semiflexible wormlike polymer to the surface of a flat wall by a square potential well of width W and depth v . Using a wormlike chain formalism that couples the orientational and positional degrees of freedom, for a wormlike chain much longer than the persistence length, we numerically calculate the adsorption phase diagram and analyze the scaling behavior near the phase transition. Our numerical results over a wide range of W can be used to identify scaling behaviors valid in the large and small width-to-persistence-length ratio as well as near the adsorption phase transition. © 2010 American Institute of Physics.

[doi:10.1063/1.3452322]

I. INTRODUCTION

Theoretical understanding of the properties of a polymer near a flat surface or interface is a topic that has generated much interest because of its relevance in practical systems.¹ For the problem of a flexible polymer of the Kuhn length a attracted to a short-ranged potential well of the force range W , it has been long established that the adsorption transition takes place at²

$$\beta v_c = D_0(a/W)^2, \quad (1)$$

where no excluded-volume interactions between polymer segments are assumed and v_c is the critical potential-well depth beyond which an adsorbed state is stabilized. Here, $\beta = 1/k_B T$, k_B is the Boltzmann constant, and T is the temperature of the system; D_0 is a numerical constant that depends on the potential model considered. Theoretically, one can use a Gaussian distribution function to describe the polymer statistics to arrive at this result.³ The typical assumption is that the physical details in a length scale smaller than the Kuhn length are neglected, which means that the result is only valid in the parameter regime $a \leq W$.

A wormlike (or semiflexible) polymer is characterized by the bare persistence length ℓ_p ,³⁻⁵ which, based on the definition of the end-to-end distance, can be related to the Kuhn length a by the relationship $\ell_p = a/2$ in the long polymer limit.^{4,6} The wormlike polymer model is particularly useful in understanding biological molecules, where, for example, double-stranded DNA would have a persistence length much greater than a typical force range of a short-range nature. The topic of adsorption, or sometimes termed as binding, of a semiflexible polymer has received intensive theoretical attention because of the practical application and

even just the theoretical interest by itself.⁷⁻¹³ We know, for example, when W is much less than a , the adsorption transition takes place at

$$\beta v_c = D_1(a/W)^{2/3}, \quad (2)$$

where D_1 is another numerical constant.^{8,14,15} This scaling relation is different from Eq. (1) and is expected for the parameter regime $a \gg W$.

The central focus of the current work is to provide accurate numerical results from solving a model of wormlike polymer adsorption to a square well potential near a featureless wall [see Fig. 1(a)]. The data cover a wide parameter range in W/a where the crossover from Eq. (1) to Eq. (2) can be analyzed. With such a solution, we can examine a complete adsorption phase diagram, which, of course, approaches the known scaling limits (1) and (2) in the appropriate limits. We further explore other important features of the adsorption transition, such as the order of the phase transition, as well as the scaling properties of the adsorbed monomer fraction and the free energy near the transition point. The understanding of the $W \sim a$ regime is relevant in biological systems. For example, the crossover of the two similar scaling limits for a confined wormlike polymer was recently tested experimentally by observing confined DNA molecules in a tube.¹⁶ Recent computer simulations have also explored various aspects of the adsorption problem of a wormlike chain.^{17,18}

In this paper, we start by examining a model for the adsorption problem of a wormlike chain to a hard wall through a square potential well with varying size of the width-to-Kuhn-length ratio, W/a ; the model is then solved in terms of full numerical solution to the resulting differential equation for the partition function (see Sec. II). A reader who is not interested in technical details can skip directly to Sec. III where we describe the main numerical results yielded from the model. In Sec. III A, we describe the adsorption phase diagram and analyze the associated scaling

^{a)}Electronic mail: jeffchen@uwaterloo.ca.

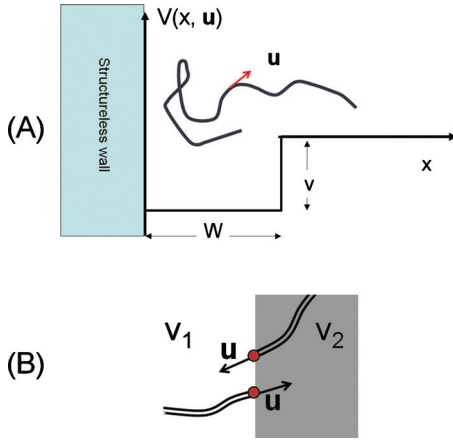


FIG. 1. (a) Schematic of a square potential well of width W and depth v near a hard wall. The normal to the surface of the flat wall is selected as the x axis. The potential energy $V(x, \mathbf{u})$ acts on a wormlike polymer segment located at x and having an orientation specified by \mathbf{u} . (b) Illustration of the \mathbf{u} dependence of the potential energy at a plane boundary where the potential energy takes a jump from v_1 to v_2 .

behavior near the transition point; in Sec. III B we then show how these results are consistent with the expected flexible-chain results in the large width limit, $W \gg a$, recovering the power law in Eq. (1); finally in Sec. III C we compare our results with previous studies in the narrow-width limit, $W \ll a$.

II. MODEL

A. Basic formalism

In the continuous description of wormlike polymer statistics by Saitô *et al.*,⁴ the configuration of a polymer of length L is described by a space curve $\mathbf{r}(t)$, where t is an arc variable which has the value 0 and L/a at the starting and terminal ends of the polymer. The statistical weight depends on the local curvature variation and an external potential,

$$P \propto \exp \left[- \int_0^{L/a} dt \left\{ \frac{1}{4} \left| \frac{d\mathbf{u}(t)}{dt} \right|^2 + \beta V[\mathbf{r}(t), \mathbf{u}(t)] \right\} \right], \quad (3)$$

where $\mathbf{u}(t)$ is a unit vector $\mathbf{u}(t) \equiv (1/a) d\mathbf{r}(t)/dt$ and $V(\mathbf{r}, \mathbf{u})$, a function of both \mathbf{r} and \mathbf{u} , is the external potential acting on a segment of length a . The coefficient of the first term in the exponent can be related to the bending energy of two connected wormlike polymer portions and could be expressed in terms of the bare persistence length of a wormlike polymer chain as in the original expression of Saitô *et al.*⁴ In writing down Eq. (3), we have adopted the convention that the effective Kuhn length a is twice of the bare persistence length in order to make a direct comparison with the properties of a flexible chain; in such a convention, in free space a long wormlike chain has a mean square end-to-end distance equal to aL .

We are interested in considering a physical quantity that is a function of both x and u_x , where $u_x \equiv \cos \theta$ is the projection of the unit vector \mathbf{u} onto the x axis. For this purpose, we consider the probability function $\Psi(x, u_x; t)$ that a polymer portion of length t has an end located at x and whose tangent vector \mathbf{u} has a projection u_x . The computation of the

probability function $\Psi(x, u_x; t)$ is equivalent to solving the differential equation,⁵

$$\frac{\partial}{\partial t} \Psi(x, u_x; t) = \left[\nabla_u^2 - a u_x \frac{\partial}{\partial x} - \beta V(x, u_x) \right] \Psi(x, u_x; t), \quad (4)$$

where the initial condition,

$$\Psi(x, u_x; 0) = 1 \quad (5)$$

and $\nabla_u^2 \equiv (1/\sin \theta)(\partial/\partial \theta) \sin \theta (\partial/\partial \theta)$. The total partition function of the polymer chain Q is related to $\Psi(x, u_x; t)$ by

$$Q = \int_0^\infty dx \int d\mathbf{u} \Psi(x, u_x; L/a). \quad (6)$$

Equation (4) is written for the probability function $\Psi(x, u_x; t)$ with variables (x, u_x) in a one-dimensional system, reduced from a similar equation with the full (\mathbf{r}, \mathbf{u}) dependence.^{19–21}

In this paper we consider the long-chain limit only, i.e., we assume that the radius of gyration of the chain is much greater than both a and W ; in such a case we only need to deal with the ground-state solution for the operator in the square brackets of Eq. (4).²⁰ The probability function is approximated by

$$\Psi(x, u_x; t) \approx \Psi_0(x, u_x) \exp(-\beta \mu t) \quad (7)$$

and the partial differential equation can now be written as

$$-\beta \mu \Psi_0(x, u_x) = \left[\nabla_u^2 - a u_x \frac{\partial}{\partial x} - \beta V(x, u_x) \right] \Psi_0(x, u_x), \quad (8)$$

where mathematically $\beta \mu$ and $\Psi_0(x, u_x)$ are the ground-state eigenvalue and eigenfunction of the operator in the square brackets (multiplied by a minus sign). Taking Eqs. (6) and (7), we can then express the reduced free energy per segment, $\beta F a/L$, as

$$\begin{aligned} \beta F a/L &= -(a/L) \ln Q \\ &= \beta \mu - (a/L) \ln \left[\int_0^\infty dx \int d\mathbf{u} \Psi_0(x, u_x) \right] \\ &\approx \beta \mu + \mathcal{O}(a/L). \end{aligned} \quad (9)$$

Hence for a long chain ($L \gg a$), the eigenvalue μ is the free energy per segment or the chemical potential.

Mathematically because of the second operator in the square brackets of Eq. (8), we have $\Psi_0(x, u_x) \neq \Psi_0(x, -u_x)$; physically, because $\Psi_0(x, u_x)$ represents the un-normalized probability of finding a (long) polymer portion with the terminal end located at x and the terminal tangent vector projecting u_x , the presence of flat surfaces at $x=0$ and $x=W$ destroys the reflection symmetry of Ψ_0 when $u_x \rightarrow -u_x$. The segmental distribution function, averaged over the entire chain, for finding an internal segment of the polymer, located at x and with a tangent vector pointing at u_x , can be written as²¹

$$\begin{aligned}\rho(x, u_x) &= \frac{1}{Q} \int_0^{L/a} dt \Psi(x, u_x; t) \Psi(x, -u_x; L/a - t) \\ &= \frac{\Psi_0(x, u_x) \Psi_0(x, -u_x)}{\int dx \int d\mathbf{u} \Psi_0(x, u_x)}.\end{aligned}\quad (10)$$

Note that the internal segmental distribution function maintains the symmetry $\rho(x, u_x) = \rho(x, -u_x)$.

For later use we further define the fraction of the adsorbed segments in the potential well,

$$\rho_{\text{in}} = \int_0^{W/a} dx \int d\mathbf{u} \rho(x, u_x) / \int_0^\infty dx \int d\mathbf{u} \rho(x, u_x). \quad (11)$$

Because of the fact that $\rho(x, u_x)$ in Eq. (10) is normalized to 1, we only need to carry out the calculation for the numerator in above definition.

Next we consider an expression for the square potential well in the problem. Normally we would write

$$V(x, u_x) = \begin{cases} 0 & \text{if } \infty > x > W \\ -v & \text{if } W > x > 0 \\ v_\infty & \text{if } 0 > x, \end{cases} \quad (12)$$

where $v_\infty = \infty$ and is actually represented by a large positive number in numerical implementation of the problem. The u_x dependence of the potential function shows up at plane boundaries $x=0$ and $x=W$ only. Consider a polymer segment represented by the hollow line and a terminal monomer represented by the circle in Fig. 1(b). At the boundary, the monomer with the rest of the polymer segment in the v_2 region is accompanied by a directional vector \mathbf{u} pointing in the negative x direction ($u_x < 0$); hence at the boundary the potential energy acting on this monomer is v_2 . From an opposite perspective, at the same boundary, a monomer with a \mathbf{u} pointing in the positive x direction ($u_x > 0$) experiences a potential energy v_1 . Using this argument for the wall boundary at $x=0$, where $v_1 = v_\infty$ and $v_2 = -v$, we have

$$\beta V(0, u_x) = \begin{cases} -v & \text{if } u_x < 0 \\ v_\infty & \text{if } u_x \geq 0. \end{cases} \quad (13)$$

Such a wall potential was considered previously for the treatment of wormlike polymers in similar physical circumstances.^{22,23} Using the same argument but now for the well boundary $x=W$, where $v_1 = -v$ and $v_2 = v_0 = 0$, we can write

$$\beta V(W, u_x) = \begin{cases} -v & \text{if } u_x > 0 \\ v_0 = 0 & \text{if } u_x \leq 0. \end{cases} \quad (14)$$

An interesting special case of the above expression is to mathematically take $v_0 = v_\infty$ instead of 0, which physically represents another hard wall at $x=W$; using the same formalism and numerical scheme, one of us considered such a slit-potential problem for a wormlike chain in a previous work.¹⁹ The orientational dependence of the potential well, $V(x, u_x)$, is a complication in treating a wormlike polymer problem, which is not a concern in the treatment of the adsorption problem of a Gaussian chain.

The application of the differential equation (8) to the adsorption problem was previously considered

theoretically,^{7,8,10,13} where the form of the potential well, in particular, the type of the force range, was also a major concern. In this work, we pay attention to a square potential well only.

In summary, defining $\tilde{x} = x/W$ and examining the form of the potential function, we can see that Eq. (8) contains two parameters: W/a and βv . To determine the adsorption transition of a wormlike polymer in a square well potential, we need to solve the eigenproblem in Eq. (8). The adsorbed state has the physical characteristics that ρ_{in} in Eq. (11) is nonzero and the reduced free energy per segment $\beta\mu$ is lower than zero.

B. Numerical treatment

The numerical scheme used to solve the differential equation (8) is based on a truncated Legendre expansion for the u_x variation of the function $\Psi_0(x, u_x)$,

$$\Psi_0(x, u_x) = \sum_{l=0}^L \Phi_l(\tilde{x}) P_l(u_x), \quad (15)$$

where $P_l(u_x)$ is the l th rank Legendre polynomial of u_x . Multiplying the left- and right-hand sides of Eq. (8) by a Legendre polynomial and integrating over u_x , we rewrote the differential equation in terms of coupled differential equations for the unknown $\Phi_l(\tilde{x})$, $l=0, 1, 2, 3, \dots, L$. In practice we kept terms up to the rank $L=16$. The truncation error was estimated by an examination of the solution in comparison with that based on a series composed of terms containing $L=14$ Legendre polynomials or lower; estimated numerical errors presented in the illustrations of this work are smaller than the size of symbols.

For the \tilde{x} dependence in the function $\Psi_l(\tilde{x})$, we simply divide the space in x by M nonuniform parts, setting up more divisions near the regions $\tilde{x}=0$ and $\tilde{x}=1$ because we expect that the functions make more drastic changes in these areas. The derivative with respect to x in Eq. (8) was treated by a forward difference at $x=0$ and a central difference for all other data points. In total, $M=8 \times 10^3$ divisions in \tilde{x} and a range of $\tilde{x}=[0, 10^4]$ was considered in our computation.

Within this numerical scheme, we can organize the numerical representation of $\Psi_l(\tilde{x})$ by a vector that contains a block of $L+1$ variables for every point in x . This way, the operator associated with the square bracket can be formatted into a tridiagonal block matrix form, each block matrix having $(L+1) \times (L+1)$ variables. We then deal with a matrix eigenproblem, where the matrix is of the dimension $N \times N$ where $N=(L+1)M$. Similar numerical approaches have been previously used for solving partial differential equations to study the isotropic-nematic interface of liquid-crystal system composed of wormlike polymers,²⁴ the surface orientational wetting transition of wormlike polymers,²² and the structure and surface phase transitions of wormlike chains confined between two walls.^{19,25,26} The Legendre-function expansion for the current problem has been used in related systems^{27,28} and is a simpler version of an expansion based on the spherical harmonics.^{22,24,25}

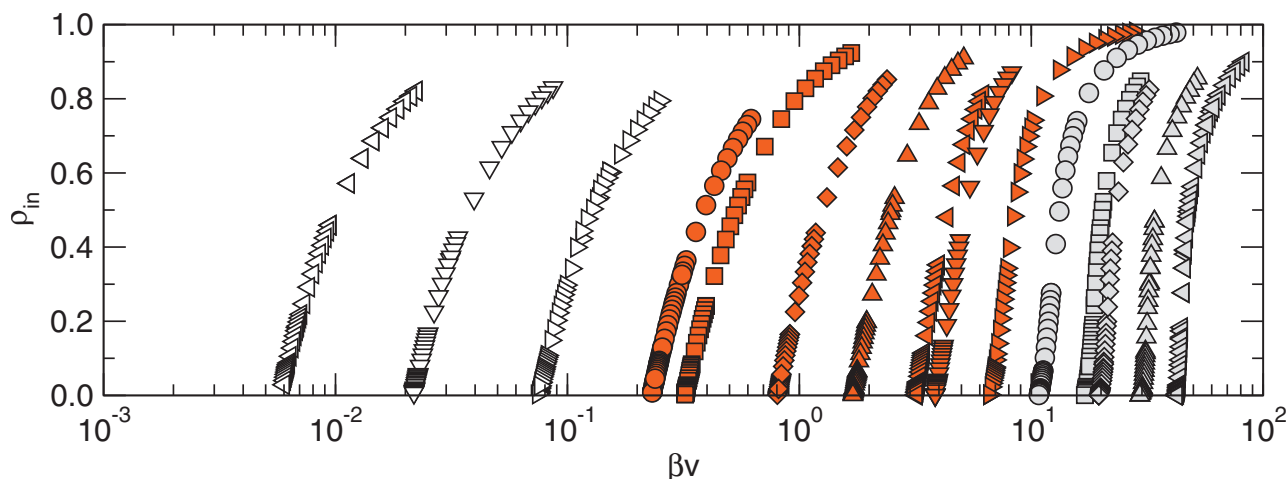


FIG. 2. Numerical results for the segment fraction inside the potential well, ρ_{in} , as a function of the reduced potential-well depth βv for various values of W/a , the ratio between potential-well width, and the effective Kuhn length of a long wormlike polymer. The profiles have been plotted by using symbols of three types of filling colors. The three sets of open symbols, left, down, and right triangles, correspond to potentials having width $W/a=8, 4$, and 2 , respectively. The seven sets of symbols in red circles, squares, diamonds, up triangles, left triangles, down triangles, and right triangles correspond to $W/a=1, 0.8, 0.4, 0.2, 0.1, 0.08$, and 0.04 , respectively. Finally, the five sets of symbols in light gray circles, squares, diamonds, up triangles, and left triangles correspond to $W/a=0.02, 0.01, 0.008, 0.004$, and 0.002 , respectively.

III. RESULTS AND DISCUSSION

We demonstrated in the last section that the state of the adsorbed wormlike chain is determined by two parameters: the ratio between the force range of the potential and the relative Kuhn length of the wormlike polymer, W/a , and the reduced potential-well depth, βv . For various ratios W/a , we change βv and measure the adsorption fraction, $\rho_{in}(W/a, \beta v)$, from strong adsorption where ρ_{in} is close to one to the near-transition region, where ρ_{in} approaches zero. The original data for $\rho_{in}(W/a, \beta v)$ are displayed in Fig. 2, for W/a in the range $[0.002, 8]$. Most data with open symbols are in a scaling regime that can be described by the scaling law of the adsorption problem of a flexible (Gaussian) polymer chain to be further discussed in Sec. III B. Most symbols filled with light gray color are in a scaling region where we expect a different scaling behavior to be discussed in Sec. III C. Symbols filled with red colors are in a crossover regime.

A. Phase diagram and scaling laws

The fact that the adsorption transition of a flexible polymer to a surface with a short-range attraction is a second-order phase transition is now well established. As a result, going from the adsorbed state, the adsorbed fraction of segments, ρ_{in} , as a function of βv intersects the βv axis at the transition point βv_c linearly.²

For illustration purpose, sets of numerical data of the adsorbed segment fraction for various values of W/a are plotted in Fig. 2 with a semilogarithmic scale. In actual numerical analysis, we used linear-linear plots (not shown) for each individual values of W/a . Those symbols with open and red symbols can be seen to linearly approach the phase transition point, where $\rho_{in}=0$. This offers a method for numerical determination of the transition point $\beta v_c(W/a)$. We have followed the data points with ρ_{in} less than 0.1 for this purpose. The data for the adsorbed segment fraction in gray-filled

symbols behave linearly only in the close vicinity of the transition; after zooming into this region, we also estimated the transition point.

The numerical results for the phase transition between the desorbed and adsorbed states based on an analysis of the adsorption fraction are displayed in Fig. 3. We also plotted a solid phase boundary curve $\beta v_c(W/a)$ by an interpolation of the numerical data in circles. Within four orders of magnitude in the graph, we can empirically capture the data by

$$\beta v_c(W/a) = \frac{(\pi^2/24)(a/W)^2}{[C_2(a/W)^2 + C_1(a/W) + 1]^{2/3}}, \quad (16)$$

where the coefficients $C_2=0.383\,05$ and $C_1=0.938\,78$ were fitted to data points shown in the figure.

To demonstrate the linearity of ρ_{in} near the transition point,²

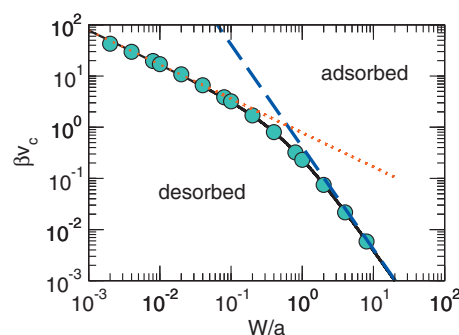


FIG. 3. Numerical solution for the reduced critical potential-well depth βv_c , represented by circles, at the phase boundary between adsorbed and desorbed phases, as a function of the potential-well width to the effective Kuhn length ratio: W/a . The dashed line and dotted lines indicates asymptotic scaling laws in the large and small W/a regions. The solid curve represents the empirical formula for the entire phase boundary, Eq. (16), that interpolates the numerical data.

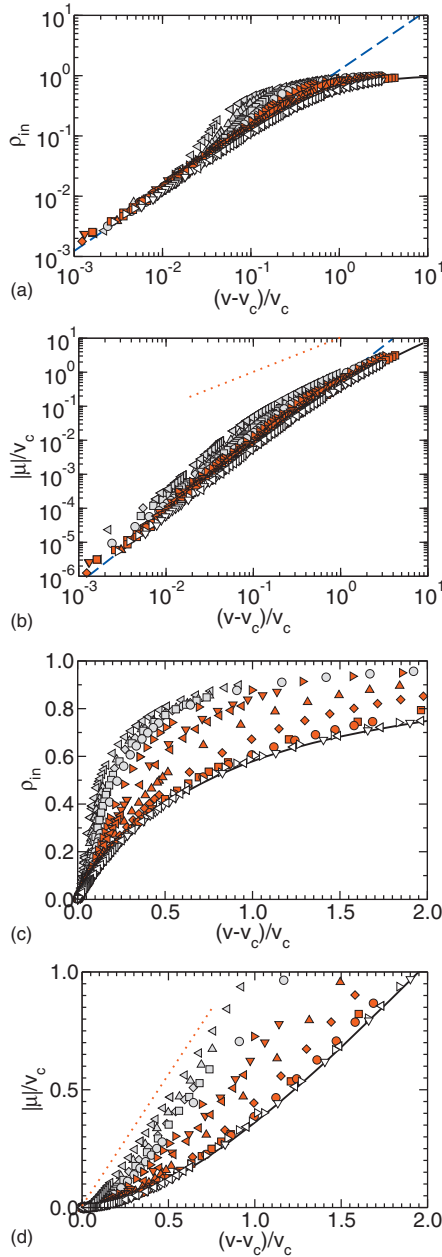


FIG. 4. Double logarithmic plots of (a) the adsorption fraction, ρ_{in} , and (b) the free energy per segment, $\beta\mu$, as a function of $(v-v_c)/v_c$ for various values of W/a . The symbols have the same meaning as those explained in the figure caption of Fig. 2. The same quantities are also plotted in linear scale in (c) and (d). Imposing on the plots are the full solution to the $W/a \gg 1$ case (solid curves), the scaling behavior of the $W/a \gg 1$ case near the critical point (dashed lines), and the expected scaling behavior of the $W/a \ll 1$ limit (dotted lines).

$$\rho_{in}(W/a, \beta v) \propto (v/v_c - 1) \quad [(v/v_c - 1) \ll 1], \quad (17)$$

we show $\rho_{in}(W/a, \beta v)$ as a function of $v/v_c - 1$ in a double logarithmic plot in Fig. 4(a). Furthermore, a dashed line representing a slope of 1 has also been included. All data collapse and approach a single scaling power law shown in Eq. (17). It can be observed that large and medium W/a cases (open and red symbols) have relatively large critical region, whereas smaller W/a cases (gray filled symbols) have a progressively reduced critical region, probably diminishing at $W/a=0$.

This analysis, wherein the numerical data for the adsorbed segment fraction follows power law (17), establishes that the adsorption transition for all W/a considered in this work is second order, similar to the case for large W/a (well known in literature). The only exception is probably the extremely small W/a limit.¹⁵ Another somewhat surprising feature of the scaling behavior of Fig. 4(a) in the small $v/v_c - 1$ region is the lack of W/a dependence in that limit. The power law (17) may contain a W/a dependence as the prefactor on the right-hand side, which would show up in Fig. 4(a) as a series of parallel lines for various W/a , all having a slope of 1 in the double logarithmic plot.

To confirm the second-order nature of the transition, we further examine the dependence of the free energy per segment, μ , as a function of $v/v_c - 1$ near the transition point. For a second-order transition, we expect that

$$-\mu(W/a, \beta v)/v_c \propto (v/v_c - 1)^2, \quad (18)$$

near the critical point $(v/v_c - 1) \ll 1$. The power-law exponent 2 is a signature of the second-order transition. Figure 4(b) demonstrates that all W/a cases display the above power law in the small $v/v_c - 1$ region; for comparison, a dashed line has been drawn with the anticipated power-law exponent 2 (the middle part of the dashed line is blocked by symbols in the plot). The critical regions for the gray symbols, judged from the agreement with the slope of 2, are much smaller, consistent with the scaling analysis of the adsorption fraction. In small W/a cases, also noticeable in the figure is that the numerical data for the μ/v_c curves show a series of W/a dependent straight lines in the small $v/v_c - 1$ region, indicating that there is a W/a dependence in the prefactor on the right-hand side of Eq. (18), as fully expected.

B. Recovery of the flexible-chain results in $W \gg a$

As a common feature in wormlike chain systems, in the $W/a \gg 1$ limit, the formalism established above recovers the Gaussian-chain formalism. For the current problem, the proof is almost identical to that given in Sec. III of a recent publication by Chen and Sullivan;¹⁹ here we outline the main steps only.

We consider a Legendre expansion for the u_x variation of the function $\Psi_0(\tilde{x}, u_x)$,

$$\Psi_0(\tilde{x}, u_x) = \sum_{l=0}^{\infty} \Phi_l(\tilde{x}) P_l(u_x). \quad (19)$$

Inserting this expression to the differential equation for the region $\tilde{x} > 1$, we obtain a series of coupled equations containing $\Phi_l(\tilde{x})$ s,

$$\beta\mu\Phi_0(\tilde{x}) = \frac{1}{3} \frac{a}{W} \frac{d}{d\tilde{x}} \Phi_1(\tilde{x}) \quad (20)$$

and

$$\begin{aligned}\beta\mu\Phi_l(\tilde{x}) = & l(l+1)\Phi_l(\tilde{x}) + \frac{l}{2l-1} \frac{a}{W} \frac{d}{d\tilde{x}} \Phi_{l-1}(\tilde{x}) \\ & + \frac{l+1}{2l+3} \frac{a}{W} \frac{d}{d\tilde{x}} \Phi_{l+1}(\tilde{x}),\end{aligned}\quad (21)$$

for $l \geq 1$. For the region $0 < \tilde{x} < 1$ we obtain a similar set of equation as the two above, the only difference being that μ is replaced by $\mu + v$. Going through the same proof as in Ref. 19, we finally arrive at

$$\beta\mu\Phi_0(\tilde{x}) = - \left[\frac{1}{6} \left(\frac{a}{W} \right)^2 \frac{d^2}{d\tilde{x}^2} \right] \Phi_0(\tilde{x}) + \mathcal{O} \left(\frac{a}{W} \right)^4 \quad (22)$$

for $\tilde{x} > 1$ and

$$\beta\mu\Phi_0(\tilde{x}) = - \left[\frac{1}{6} \left(\frac{a}{W} \right)^2 \frac{d^2}{d\tilde{x}^2} + \beta v \right] \Phi_0(\tilde{x}) + \mathcal{O} \left(\frac{a}{W} \right)^4, \quad (23)$$

for $0 < \tilde{x} < 1$. To proceed further we note that $\beta\mu \sim (a/W)^2$ and the parameter region $\beta v \lesssim (a/W)^2$ is our main concern; these order-of-magnitude considerations will be self-consistently verified in the next few paragraph. Neglecting terms of order $(a/W)^4$ we see that the last two equations are identical to the square well adsorption problem of a Gaussian chain.³

We note the following known features of the solution to the eigenproblem in Eqs. (22) and (23), after dropping all $\mathcal{O}(a/W)^4$ terms. An adsorption of the polymer takes place as βv goes beyond a critical point βv_c , where βv_c has a power law given in Eq. (1),

$$\beta v_c = (\pi^2/24)(a/W)^2. \quad (24)$$

The dashed line in Fig. 3 represents this power law including the prefactor $\pi^2/24$, completely agreeing with the numerical data in the large W/a limit. We used the coefficient $\pi^2/24$ explicitly in our empirical formula (16) for interpolation purpose.

Beyond but close to the critical point $v/v_c \gtrsim 1$, we can show that the solution to Eqs. (22) and (23) gives the free energy per segment,

$$\frac{\mu}{v_c} = \frac{\pi^2}{48} \left(\frac{v - v_c}{v_c} \right)^2 + \mathcal{O} \left[\left(\frac{v - v_c}{v_c} \right)^3, \left(\frac{a}{W} \right)^2 \right], \quad (25)$$

and the fraction of adsorbed polymer segments,

$$\rho_{\text{in}} = \frac{\pi^2}{8} \left(\frac{v - v_c}{v_c} \right) + \mathcal{O} \left[\left(\frac{v - v_c}{v_c} \right)^2, \left(\frac{a}{W} \right)^2 \right]. \quad (26)$$

These results are demonstrated by blue dashed lines in Figs. 4(a) and 4(b) and have been known results for flexible polymer adsorption.² These power laws agree with our numerical data in the phase transition region.

A more careful full numerical treatment of the eigenproblem in Eqs. (22) and (23) that goes beyond the leading terms in $v/v_c - 1$ can also be done; the resulting ρ_{in} and $\beta\mu$ are displayed in Fig. 4 by solid curves, with an error of $(a/W)^2$ inherited from these equations. We can see that the numerical data for large W/a , especially those with open symbols, agree well not only with the near-critical results (25) and (26) but those *full* solutions as well.

A similar discussion of the recursion relation in Eq. (21), but in a different context, not involving the width W , on recovering the Gaussian limit, was previously described by Schmid and Müller.²⁹ Morse and Fredrickson³⁰ also discussed this briefly for the interface problem of a polymer mixture.

In the above discussions, we showed that the wormlike chain adsorption problem recovers the Gaussian-chain adsorption problem in the limit of $a/W \ll 1$, and that the second-order differential equation for $\Phi_0(\tilde{x})$, Eqs. (22) and (23), respectively, for the two regions in \tilde{x} , is identical in both problems. One apparent contradiction is the boundary conditions at $\tilde{x}=1$ (or $x=W$): associate with the Gaussian-chain problem [Eqs. (22) and (23) without terms $\mathcal{O}(a/W)^4$], we know that the first derivative of $\Phi_0(\tilde{x})$ must be *continuous* across the boundary; on the other hand, Eq. (8), or its equivalent expanded form Eq. (21), contains a first derivative, $\partial\Phi/\partial x$, which implies that the first derivative is *discontinuous* at the boundary. Indeed, iteratively through Eq. (21) by an order-of-magnitude estimate, we can show that

$$\Phi_l(\tilde{x}) \sim \mathcal{O}(a/W)^l \quad (27)$$

and

$$\Phi'_l(\tilde{x}=1+0) - \Phi'_l(\tilde{x}=1-0) \sim \mathcal{O}(a/W)^{l+2}, \quad (28)$$

where the prime represents the first derivative with respect to \tilde{x} . Hence, the first derivative of the probability function Ψ in \tilde{x} is discontinuous. The connection to the Gaussian-chain adsorption problem can be made by realizing that at the boundary $x=W$ the discontinuity in $\Phi'_0(\tilde{x})$ is of order $\mathcal{O}(a/W)^2$, which vanishes in the “true” Gaussian limit, $a/W \sim 0$, rendering a continuous change in the first derivative across the boundary at $x=W$.

C. The asymptotic case of $W \ll a$

The other important limit is $W \ll a$, when the persistence length of the wormlike polymer is much greater than the potential-well width. This is not uncommon in biological systems, where, for example, the persistence length of a long DNA chain can be a few order of magnitude larger than a typical force range in the system. On the basis of a scaling argument comparing energetics and entropies in the system, Semenov¹⁵ recently argued that the adsorption transition takes place following the power law in Eq. (2), in consistency with an earlier suggestion by Maggs *et al.*¹⁴ Our numerical data, or the empirical representation (16) in the small W/a limit, $(\pi^2/24)[C_2 W/a]^{-2/3}$ (shown as the dotted line in Fig. 3), agree well with the expected power law in Eq. (2).

Semenov¹⁵ suggested that for all W/a except for $W/a = 0$, the adsorption phase transition of a wormlike chain to a square well is second order, which is verified by our numerical solution in Sec. III A; he has also indicated that in the extreme limit $W/a \rightarrow 0$, the transition becomes sharper and finally approach a first-order one at $W/a = 0$. In the $W/a \rightarrow 0$ case, the first-order nature of the adsorption transition driven by a short-ranged surface force (or regarded as unbinding transition if one starts with an adsorbed state) was also explored and concluded by Maggs *et al.*¹⁴ as well as

Gompper and Burkhardt.⁷ Our numerical scheme is limited to W/a as small as 0.002 and we have not found an accurate numerical method to directly reach the $W/a=0$ limit. In a linear plot, we observe that $\rho_{\text{in}}(W/a, \beta v)$ for small W/a , shown in Fig. 4(c) by gray symbols, has an increasing tendency of becoming a step function near v_c as W/a decreases. Another property of the first-order nature at $W/a=0$ is that the free energy per segment is expected to display a linear behavior in $v/v_c - 1$ rather than the quadratic behavior in Eq. (18).¹³ We have imposed a linear dotted line, in both Figs. 4(b) and 4(d), for comparison. From these plots there is a good suggestion that in the $W/a=0$ limit the second-order region shrinks to zero and a first-order region takes over. Semenov¹⁵ further proposed an expression for $\mu(W/a, \beta v)$, which qualitatively contains the desirable features of the free energy over the entire W/a regime, including the crossover to a first-order behavior in the limit $W/a \rightarrow 0$ [his Eq. (32)]. We have attempted but unable to quantitatively verify the validity of this expression against our numerical solutions.

In an attempt to solve the current adsorption problem, Kuznetsov and Sung^{31,32} started from the same differential equation, Eq. (8), and followed by considering the two truncated equations, similar to Eq. (20) for the zeroth order and Eq. (21) for a perturbation correction. Generalizing these two equations to the entire W/a region, large and small, they found yet another first-order transition line in the phase region labeled “adsorption” in our phase diagram (Fig. 3). We have not found the validity of such a claim in comparison with our full numerical treatment.

Burkhardt²³ considered a solution to Eq. (8) for a wormlike polymer confined in a narrow rectangular tube where two directions along the sides of the rectangle can be variable separated. Focusing on one of the two directions, we can take his result and regard it as a solution for a wormlike chain confined by parallel plates where $W \ll a$; the free energy per segment, f , is then scaled by $\beta f = A(a/W)^{2/3}$, where A is a numerical constant.^{33,34} Returning to our current adsorption problem, we can push the limit of βv to $+\infty$ and the current adsorption problem becomes a confinement problem.¹⁹ We see the connection between these two problems through how the energetics in these two problems are all scaled by the same $(a/W)^{2/3}$ power laws. This connection was considered by Maggs *et al.*¹⁴ in an analysis of Eq. (8) for the $W \gg a$ region.

IV. SUMMARY

In summary, we considered a full numerical solution to the ground-state dominating problem for the adsorption of a wormlike polymer chain to a square well potential of depth v and width W . We have numerically computed the adsorption

density and the free energy per segment as a function of the reduced potential depth, βv , in the crossover regime between the two scaling limits, $W \gg a$ and $W \ll a$, where a is the effective Kuhn length. Analyzing the adsorption data for the range of W/a considered in this work, we calculated the adsorption phase diagram and found that the phase transition is second order. Our data also support the conclusion that the second-order region reduces in size as we take the $W/a \rightarrow 0$ limit, eventually replaced by a first-order behavior at $W/a=0$.

ACKNOWLEDGMENTS

We wish to thank the NSERC for financial support and the SHARCNET for computation time.

- ¹R. R. Netz and D. Andelman, *Phys. Rep.* **380**, 1 (2003).
- ²P.-G. de Gennes, *Rep. Prog. Phys.* **32**, 187 (1969).
- ³M. Doi and S. F. Edwards, *The Theory of Polymer Dynamics* (Oxford University Press, New York, 1988).
- ⁴N. Saitô, K. Takahashi, and Y. Yunoki, *J. Phys. Soc. Jpn.* **22**, 219 (1967).
- ⁵K. F. Freed, *Adv. Chem. Phys.* **22**, 1 (1972).
- ⁶O. Kratky and G. Porod, *Recl. Trav. Chim. Pays-Bas* **68**, 1106 (1949).
- ⁷G. Gompper and T. W. Burkhardt, *Phys. Rev. A* **40**, 6124 (1989).
- ⁸G. Gompper and U. Seifert, *J. Phys. A* **23**, L1161 (1990).
- ⁹C. C. van der Linden, F. A. M. Leermakers, and G. J. Fleer, *Macromolecules* **29**, 1172 (1996).
- ¹⁰T. W. Burkhardt, *J. Phys. A* **33**, L429 (2000).
- ¹¹S. Stepanow, *J. Chem. Phys.* **115**, 1565 (2001).
- ¹²P. Benetatos and E. Frey, *Phys. Rev. E* **67**, 051108 (2003).
- ¹³J. Kierfeld and R. Lipowsky, *J. Phys. A* **38**, L155 (2005).
- ¹⁴A. C. Maggs, D. A. Huse, and S. Leibler, *Europhys. Lett.* **8**, 615 (1989).
- ¹⁵A. N. Semenov, *Eur. Phys. J. E* **9**, 353 (2002).
- ¹⁶W. Reisner, K. J. Morton, R. Riehn, Y. M. Wang, Z. Yu, M. Rosen, J. C. Sturm, S. Y. Chou, E. Frey, and R. H. Austin, *Phys. Rev. Lett.* **94**, 196101 (2005).
- ¹⁷T. Sintes, K. Sumithra, and E. Straube, *Macromolecules* **34**, 1352 (2001).
- ¹⁸V. A. Ivanov, J. A. Martemyanova, M. Müller, W. Paul, and K. Binder, *J. Phys. Chem. B* **113**, 3653 (2009).
- ¹⁹J. Z. Y. Chen and D. E. Sullivan, *Macromolecules* **39**, 7769 (2006).
- ²⁰A. Yu. Grosberg and A. R. Khokhlov, *Statistical Physics of Macromolecules* (American Institute of Physics, New York, 1994).
- ²¹G. H. Fredrickson, *The Equilibrium Theory of Inhomogeneous Polymers* (Oxford University Press, New York, 2006).
- ²²Z. Y. Chen and S. M. Cui, *Phys. Rev. E* **52**, 3876 (1995).
- ²³T. W. Burkhardt, *J. Phys. A* **30**, L167 (1997).
- ²⁴S. M. Cui, O. Akcakir, and Z. Y. Chen, *Phys. Rev. E* **51**, 4548 (1995).
- ²⁵J. Z. Y. Chen, D. E. Sullivan, and X. Yuan, *Europhys. Lett.* **72**, 89 (2005).
- ²⁶J. Z. Y. Chen, D. E. Sullivan, and X. Yuan, *Macromolecules* **40**, 1187 (2007).
- ²⁷R. C. Hidalgo, D. E. Sullivan, and J. Z. Y. Chen, *Phys. Rev. E* **71**, 041804 (2005).
- ²⁸R. C. Hidalgo, D. E. Sullivan, and J. Z. Y. Chen, *J. Phys.: Condens. Matter* **19**, 376107 (2007).
- ²⁹F. Schmid and M. Müller, *Macromolecules* **28**, 8639 (1995).
- ³⁰D. C. Morse and G. H. Fredrickson, *Phys. Rev. Lett.* **73**, 3235 (1994).
- ³¹D. V. Kuznetsov and W. Sung, *J. Chem. Phys.* **107**, 4729 (1997).
- ³²D. V. Kuznetsov and W. Sung, *Macromolecules* **31**, 2679 (1998).
- ³³T. Odijk, *Macromolecules* **16**, 1340 (1983).
- ³⁴T. Odijk, *Macromolecules* **19**, 2313 (1986).